British Journal of Pharmacology (2004) 143, 119–131
www.nature.com/bjp

$P2X_2$ and $P2Y_1$ immunofluorescence in rat neostriatal medium-spiny projection neurones and cholinergic interneurones is not linked to respective purinergic receptor function

[1]Peter Scheibler, [1]Mihail Pesic, [1]Heike Franke, [1]Robert Reinhardt, [1]Kerstin Wirkner, [1]Peter Illes & *,[1]Wolfgang Nörenberg

[1]Rudolf-Boehm-Institute of Pharmacology and Toxicology, University of Leipzig, Härtelstraße 16-18, D-04107, Germany

1 The presence of ionotropic P2X receptors, targets of ATP in fast synaptic transmission, as well as metabotropic P2Y receptors, known to activate K^+ currents in cultured neostriatal neurones, was investigated in medium-spiny neurones and cholinergic interneurones contained in neostriatal brain slices from 5–26-day-old rats.

2 In these cells, adenosine-5′-triphosphate (ATP) (100–1000 μM), 2-methylthioadenosine-5′-triphosphate (2MeSATP), α,β-methyleneadenosine-5′-triphosphate (α,βmeATP, 30–300 μM, each) and adenosine-5′-*O*-(3-thiotriphosphate (ATPγS) (100 μM) failed to evoke P2X receptor currents even when 8-cyclopentyl-1,3-dipropylxanthine (DPCPX, 0.1 μM), apyrase (10 U ml^{-1}) or intracellular Cs^+ was used to prevent occluding effects of the ATP breakdown product adenosine, desensitisation of P2X receptors by endogenous ATP and an interference with the activation of K^+ channels, respectively. P2X receptor agonists were also ineffective in outside-out patches withdrawn from the brain slice tissue. Muscimol (10 μM) evoked $GABA_A$ receptor-mediated currents under all these conditions.

3 When used as a control, locus coeruleus neurones responded with P2X receptor-mediated currents to ATP (300 μM), 2MeSATP and α,βmeATP (100 μM, each).

4 ATP and adenosine-5′-diphosphate (ADP) (100 μM, each) did not activate K^+ currents in the neostriatal neurones.

5 Despite the observed lack of function, $P2X_2$ and $P2Y_1$ immunofluorescence was found in roughly 50% of the medium-spiny neurones and cholinergic interneurones.

6 A role of ATP in synaptic transmission to striatal medium-spiny neurones and cholinergic interneurones appears unlikely, however, the otherwise silent P2X and P2Y receptors may gain functionality under certain yet unknown conditions.
British Journal of Pharmacology (2004) **143,** 119–131. doi:10.1038/sj.bjp.0705916

Keywords: Caudate–putamen; electrophysiology; immunohistochemistry; locus coeruleus; neostriatum; P2X receptors; $P2X_2$ receptors; $P2X_4$ receptors; P2Y receptors; $P2Y_1$ receptors

Abbreviations: ACSF, artificial cerebrospinal fluid; ADP, adenosine-5′-diphosphate; AHP, after-hyperpolarisation; ATP, adenosine-5′-triphosphate; ATPγS, adenosine-5′-*O*-(3-thiotriphosphate); DPCPX, 8-cyclopentyl-1,3-dipropylxanthine; EC_{50}, effective concentration evoking 50% of maximum response; ER, endoplasmic reticulum; IF, immunofluorescence; LA cell, long-lasting after-hyperpolarisation cell; LC, locus coeruleus; LY, Lucifer yellow; MAP2, microtubule-associated protein 2; 2MeSATP, 2-methylthioadenosine-5′-triphosphate; α,βmeATP, α,β-methyleneadenosine-5′-triphosphate; MS cell, medium-spiny cell; PPADS, pyridoxalphosphate-6-azophenyl-2′,4′-disulphonic acid; TTX, tetrodotoxin

Introduction

Adenosine-5′-triphosphate (ATP) is a neurotransmitter or cotransmitter acting *via* two distinct families of P2 receptors, P2X receptors, ATP-gated cation channels involved in fast synaptic transmission, as well as G protein-coupled P2Y receptors, which may participate in slow signalling in the central nervous system (Khakh, 2001). Seven different mammalian P2X receptor subunits ($P2X_{1–7}$) and eight different mammalian P2Y receptors ($P2Y_{1–2}$, $P2Y_4$, $P2Y_6$, $P2Y_{11–14}$) have been cloned to date (Burnstock, 2001; Abbracchio *et al*., 2003). The action of ATP is terminated by diffusion from its receptors and by a rapid breakdown through a cell surface located ecto-enzyme cascade (Zimmermann, 1999). It is noteworthy that the breakdown product adenosine can modulate neuronal functions by its own set of adenosine (P1) receptors (Burnstock, 2001).

In rat brain slices, a transmitter- or cotransmitter role for ATP has been conclusively proven in the medial habenula (Edwards *et al*., 1992), the nucleus locus coeruleus (LC) (Nieber *et al*., 1997), the CA1 region of the hippocampus (Pankratov *et al*., 1998) and eventually in layer II and III of the somato-sensory cortex (Pankratov *et al*., 2002), by the discovery of fast P2X receptor-mediated synaptic currents or potentials. However, ATP may serve as a mediator of

*Author for correspondence; E-mail: noerw@medizin.uni-leipzig.de

neuro – neuronal signalling in a far broader range of brain areas because P2X subunit mRNAs or P2X subunit proteins (reviewed in Nörenberg & Illes, 2000), as well as P2Y receptor mRNAs and P2Y receptor proteins (reviewed in Illes & Ribeiro, 2004), were found throughout the brain.

In the rat caudate–putamen (neostriatum), the mRNAs for $P2X_1$, $P2X_2$, $P2X_4$ and $P2X_6$ receptor subunits have been autoradiographically detected (Kidd *et al*., 1995; Collo *et al*., 1996) and, moreover, immunostaining with specific antibodies has indicated that at least $P2X_2$ and $P2X_4$ were indeed translated into receptor subunit proteins (Lê *et al*., 1998; Kanjhan *et al*., 1999). Similarly, P2Y receptor mRNAs ($P2Y_1$, $P2Y_2$, $P2Y_4$, $P2Y_6$, $P2Y_{11}$; Moore *et al*., 2001) and $P2Y_1$ receptor proteins (Moore *et al*., 2000; Franke *et al*., 2003) have been found in the caudate–putamen from humans and rats. Since, ATP was depolarisation-dependently released from cultured neostriatal neurones (Zhang *et al*., 1988), as well as synaptosomes prepared from cholinergic neostriatal interneurones (Richardson & Brown, 1987), and, because ecto-enzyme activity for the breakdown of extracellular ATP was present at least in the synaptosomes (James & Richardson, 1993), several important prerequisites for a possible neurotransmitter role of ATP in the neostriatum seem to be met.

Despite the detection of P2 receptor proteins, functional data pertaining to effects of ATP in the neostriatum are scarce. Besides ATP-induced neurotoxic effects (Ryu *et al*., 2002), it has been demonstrated only that the nucleotide, acting at pre- and postsynaptic P2Y receptors, respectively, modulated the release of dopamine in neostriatal brain slices (Trendelenburg & Bültmann, 2000) and activated a K^+ conductance in cultured neostriatal neurones (Ikeuchi & Nishizaki, 1995). Therefore, we decided to analyse soma-dendritic P2 receptor mechanisms in the rat neostriatum in some detail. In order to gain information pertaining to a possible transmitter or cotransmitter role of ATP, we searched for P2X receptor-mediated cation currents, as well as P2Y receptor-activated K^+ currents in electrophysiologically identified medium-spiny projection neurones and also in cholinergic interneurones, contained in rat neostriatal brain slices by means of the whole-cell patch-clamp technique. In addition, attempts were made to prove in the recorded neurones the presence of $P2X_2$, $P2X_4$ and $P2Y_1$ receptor subtypes by means of immunofluorescence staining with specific antibodies. A preliminary account of some of the results has appeared in abstract form (Scheibler *et al*., 2002).

Methods

Electrophysiology

Neostriatal brains slices were prepared from young 5–26-day-old Wistar rats, as previously described (Nörenberg *et al*., 1997b). This postnatal period covers the span of time during which P2X receptor activity matured in neurones of the rat LC (Wirkner *et al*., 1998). It should be noted that at least striatal medium-spiny neurones undergo profound changes in phenotype until the end of the third to fourth postnatal week including for example, the development of densely packed dendritic spines, as well as the progressive expression of inward rectifier K^+ channels (Tepper *et al*., 1998). However, the results specified later in this paper did not differ significantly when compared between neostriatal brain slices taken either from 5–7 ($n=23$), 10–14 ($n=154$) or 21–26 ($n=8$) day-old animals, and, hence, data were pooled. Pontine brain slices containing the LC were prepared from 10–14-day-old rats as previously described (Wirkner *et al*., 1998).

Experiments were carried out at room temperature in a recording chamber (300–400 μl volume) continuously superfused (3 ml min^{-1}) with artificial cerebrospinal fluid (ACSF). Neurones were visualised by means of an upright microscope ($\times 40$ water immersion objective combined with Nomarski-type differential interference contrast (DIC) optics). The ACSF had the following composition (mM): NaCl 126, KCl 2.5, NaH_2PO_4, 1.2, $CaCl_2$ 2.4, $MgCl_2$ 1.3, $NaHCO_3$ 26 and glucose 11; saturated with 95% O_2 and 5% CO_2 (pH 7.4). In some experiments, the ATP–ADPase apyrase (10 U ml^{-1}), 8-cyclopentyl-1,3-dipropylxanthine (DPCPX; 0.1 μM) or tetrodotoxin (TTX; 0.3 μM) was added to the ACSF in order to remove extracellular ATP or to suppress adenosine receptor-mediated effects and depolarisation-evoked Na^+ channel activity, respectively. In the apyrase experiments, brain slices were stored in ACSF containing the enzyme at least for 1–6 h prior to the start of recordings. In experiments with DPCPX or TTX, the compounds were added to the ACSF at least 15 min prior to the recordings and for the remainder of the experiments.

Membrane currents and membrane potentials were recorded by means of an EPC-7 patch-clamp amplifier (List Electronics, Darmstadt, Germany) using borosilicate patch pipettes (4–9 MΩ resistance) filled with an intracellular solution of the following composition (mM): K-gluconate 140, NaCl 10, $MgCl_2$ 1, HEPES 10, EGTA 11, Mg-ATP 1.5 and Li-GTP 0.3; pH 7.3 adjusted with KOH. In some experiments, an equal amount of CsCl replaced K-gluconate in order to block K^+ channel activity. The liquid junction potentials were 14.3 and 3.7 mV between the ACSF and the K-gluconate and CsCl-based pipette solutions, respectively. In experiments with the K-gluconate internal solution, membrane potential values were corrected for this amount of liquid junction potential. With the CsCl-based internal solution, no such corrections were made.

The seal resistance was between 1 and 7 GΩ. After gaining whole-cell access, the series resistance (R_s) and the associated membrane time constant were 29.6 ± 1.9 MΩ and 602.8 ± 54.9 μs, respectively. R_s did not change essentially and was 31.6 ± 2.0 MΩ at the end of the experiments ($P > 0.05$; $n=196$), indicating stable recording conditions.

Data were filtered at 1–10 kHz, digitised at 0.1–5 kHz (Model 1401) and evaluated using commercially available patch- and voltage-clamp software (both Cambridge Electronic Design, Cambridge, U.K.).

Neostriatal medium-spiny projection neurones (MS cells) and cholinergic interneurones (long-lasting after-hyperpolarisation cells, LA cells; Kawaguchi *et al*., 1995) were identified by means of combined morphological and electrophysiological criteria. To this end, the greater somatic diameter of all cells was measured under DIC optics prior to the start of experiments. In addition, the resting membrane potential, the action potential threshold and the time to the peak of the after-hyperpolarisation (AHP) of most neurones were determined under current-clamp conditions. The action potential threshold was assessed by incrementally increasing depolarising current pulses (500 ms in duration), one current pulse every 5 s, injected into the neurone under investigation, as the voltage

difference between the resting potential in the absence of current injection and the onset of the first spike. The time to peak of the AHP was the time difference between the spike onset and the voltage peak of the AHP.

LC neurones were identified within the area of the LC at the ventrolateral border of the fourth ventricle by virtue of their spontaneous action potential discharge susceptible to the inhibitory action of α_2-adrenoceptor agonists (e.g. Nörenberg *et al*., 1997a).

The presence of functional P2X receptor cation channels in neostriatal neurones, as well as LC neurones was investigated under voltage-clamp conditions at a holding potential of −80 mV. To this end, peak transmembrane current amplitudes in response to the $GABA_A$ receptor agonist muscimol (10 μM), as well as the P2X receptor agonists ATP (100–1000 μM), 2MeSATP (2-methylthioadenosine-5′-triphosphate), α,βmeATP (α,β-methyleneadenosine-5′-triphosphate; 30–300 μM, each) and, in some cases also ATPγS (adenosine-5′-*O*-(3-thiotriphosphate); 100 μM) were measured with respect to the holding current in the absence of agonists. Half-maximal effective concentrations (EC_{50}) for ATP, 2MeSATP and α,βmeATP were 1–30, 3 and >300 μM at cloned $P2X_2$ receptors and 10, 10–100 and >300 μM at cloned $P2X_4$ receptors (data taken from Khakh *et al*., 2001), for which the respective proteins have been detected in striatal neurones. ATPγS was equipotent to ATP at $P2X_2$ receptors (Brake *et al*., 1994) and roughly half as potent compared to ATP at $P2X_4$ receptors (Bo *et al*., 1995). At native P2X receptors in LC neurones, EC_{50} values for ATP, 2MeSATP and α,βmeATP were 62, 19 and 192 μM, respectively (Shen & North, 1993). Hence, the agonist concentration range used appears to be appropriate for the detection of functional P2X receptors. Agonists were consecutively pressure applied to the same neurone by means of the application cannula of a fast-flow superfusion system (Adams and List, DAD-12, NY, U.S.A.) placed near the slice surface in immediate vicinity (~100 μM) of the cell under investigation. Challenges with the individual agonists were 2 s in duration and separated by 2 min superfusion periods with drug-free ACSF. The time course of agonist application from the DAD-12 was estimated by measuring the rise times of currents elicited by the application of distilled water to the open tip of patch pipettes after experiments had finished. The time to equilibrium exchange (measured as time from 10 to 90% of the peak response) calculated from nine such trials in neostriatal brain slices was 1132±143 ms, and hence within the time limits of agonist application (2 s).

To search for P2Y receptor-mediated effects on the membrane conductance, striatal cells were voltage-clamped at a holding potential of −80 mV. Ramp depolarisations (from −140 to +40 mV at 0.18 mV ms^{-1}) were imposed two times, first in the absence and, second, after 30 s of pressure application in the continued presence of the P2Y receptor agonists ATP or adenosine-5′-diphosphate (ADP) (100 μM, each). In these experiments, voltage-activated Na^+ channels were blocked by the addition of TTX (0.3 μM) to the ACSF. EC_{50} values for ATP and ADP at rat $P2Y_1$ receptors, for which the respective protein has been detected in striatal neurones, were 140 and 9 nM, respectively (data taken from Sak & Webb, 2002). Judged from current densities, ATP (10 μM) was approximately 3–4 times more potent than ADP (10 μM) in evoking K^+ currents at native P2Y receptors in rat cultured striatal neurones (Ikeuchi & Nishizaki, 1995). Hence, the agonist concentrations used appear at all events high enough for the detection of functional $P2Y_1$ receptors.

Immunocytochemistry and confocal microscopy

The immunostaining experiments were performed in order to investigate whether the neostriatal neurones that were suitable for electrophysiological recordings were principally able to synthesise P2 receptor proteins. Since more than 80% (154 out of 185) of the electrophysiological recordings in neostriatal brain slices were made in sections taken from 10–14-day-old rats, this age group was also chosen for immunocytochemistry. Beyond that, no attempts were made to study possible effect of age on P2 receptor expression.

To accomplish the recovery of single, electrophysiologically characterised neostriatal neurones for subsequent immunostaining with $P2X_2$, $P2X_4$ and $P2Y_1$ receptor-specific antibodies, patch pipettes were filled with the intracellular K-gluconate solution also containing the fluorescent dye Lucifer yellow (LY; 1.5%). At the end of recordings, slices were fixed in paraformaldehyde (4% in 0.1 M phosphate buffer; pH 7.4) over night at 4°C. After washing in Tris-buffered saline (TBS; 0.05 M; pH 7.6), and blocking with 5% fetal calf serum (FCS) in TBS, the slices were incubated with rabbit anti-$P2X_2$, rabbit anti-$P2X_4$ or rabbit anti-$P2Y_1$ antibodies (1 : 400, each) together with 0.1% Triton X-100 in 5% FCS in TBS for 48 h at 4°C. The secondary antibody employed for the localisation of the primary P2 antisera was a Cy3-conjugated goat anti-rabbit IgG (1 : 800). After 2 h, the slices were washed three times for 5 min each in TBS, mounted on slide glasses, dehydrated in ethanol, cleared in *n*-butylacetate, embedded in entellan and capped with coverslips. When carrying out this kind of trials, the respective experimenters were unaware of the results obtained by electrophysiology.

The $P2X_2$, $P2X_4$ and $P2Y_1$ receptor distribution in rat neostriatum was also analysed in brain sections not subjected to prior electrophysiological recordings. To this end, 12-day-old Wistar rats were perfused transcardially under thiopental sodium-anaesthesia with paraformaldehyde (2%) in sodium acetate buffer (pH 6.5) followed by paraformaldehyde (2%)–glutaraldehyde (0.1%) in sodium borate buffer (pH 8.5). Then, serial coronal sections (50 μM thick) were cut containing the brain areas of interest by means of a vibratome (TSE, Bad Homburg, Germany) and collected as free-floating slices in 0.1 M Tris (pH 7.6). P2 receptor immunostaining and post-fixation of slices was essentially identical as described above, except that instead of the LY-autofluorescence, the fluorescence obtained by the combination of Cy2-conjugated goat anti-mouse IgG with the neuronal marker mouse anti-microtubule-associated protein-2 antibody (MAP2; 1 : 1000; Izant & McIntosh, 1980) was used to identify neuronal cells.

The double immunofluorescence was investigated by a confocal laser-scanning microscope (LSM 510, Zeiss, Oberkochen, Germany) equipped with an argon laser emitting at an excitation wavelength of 488 nm (yellow–green immunofluorescence: LY; Cy2) and a helium/neon laser emitting at an excitation wavelength of 543 nm (red immunofluorescence: Cy3). Only a weak background staining unrelated to identifiable neostriatal neurones was observed in control experiments when the primary $P2X_2$, $P2X_4$, $P2Y_1$ or MAP2-specific antibodies were omitted from the staining protocol or blocking peptides were used (see Figure 6j–l).

Materials

The following drugs and chemicals were used: rabbit polyclonal anti-$P2X_2$, anti-$P2X_4$ and anti-$P2Y_1$ antibodies (Alomone Labs, Jerusalem, Israel); tetrodotoxin citrate (TTX, Biotrend, Köln, Germany); mouse anti-MAP2 antibody (Chemicon, Temecula, California, U.S.A.); Cy2-conjugated goat anti-mouse IgG and Cy3-conjugated goat anti-rabbit IgG (Jackson Immuno Research, Baltimore Pennsylvania, U.S.A.); entellan (Merck, Darmstadt, Germany); FCS (Seromed, Berlin, Germany); adenosine-5′-diphosphate sodium salt (ADP), adenosine-5′-triphosphate tetrasodium salt (ATP), α,β-methyleneadenosine-5′-triphosphate dilithium salt (α,βmeATP, alternative abbreviation AMP-CPP), adenosine-5′-*O*-(3-thiotriphosphate) tetralithium salt (ATPγS), Lucifer yellow CH dilithium salt, (−)-noradrenaline bi-(+)tartrate and potato apyrase grade III (Sigma, Deisenhofen, Germany); DPCPX, 2-methylthioadenosine-5′-triphosphate tetrasodium salt (2MeSATP), pyridoxalphosphate-6-azophenyl-2′,4′-disulphonic acid tetrasodium salt (PPADS) and muscimol (Tocris Cookson, Bristol, U.K.).

Stock solutions (10–100 mM) of drugs were prepared with distilled water or dimethyl-sulphoxide in the case of DPCPX. Aliquots were stored at −20°C. Further dilutions were made daily with ACSF. Equivalent quantities of the solvent had no effect. Apyrase was directly added to the ACSF in the final concentration of 10 U ml^{-1}.

Statistics

Results are expressed throughout as means±s.e.m. of *n* individual trials. Differences between means were tested for significance by the Kruskal–Wallis ANOVA on ranks followed by Mann–Whitney *U*-test. In some cases, a modified *t*-test (Bonferroni–Dunn) for multiple comparisons was used. $P<0.05$ was the accepted level of significance.

Results

Electrophysiology: identification of neostriatal neurones

The neostriatal neurone population consists of GABAergic medium-spiny projection neurones (MS cells), large cholinergic interneurones (LA cells) and at least two classes of GABAergic interneurones with different and well-described electrophysiological properties (Kawaguchi, 1992; Kawaguchi, 1993; Kawaguchi *et al.*, 1995; Plenz & Kitai, 1998). According to the known properties of MS cells and LA cells (Table 1, right-hand columns), all neurones characterised under current-clamp conditions ($n=136$) could be divided into two groups. Cells considered to be MS neurones ($n=82$) had a relatively small soma and a strongly hyperpolarised membrane potential. They fired spikes followed by short-duration AHPs only in response to relatively strong threshold depolarisations. When supra-threshold current pulses were applied, these cells responded with trains of evenly spaced action potentials (Figure 1a; Table 1, left-hand columns).

The properties of cells considered to be LA neurones ($n=54$) differed significantly from those of the MS cells (Table 1, left-hand columns). They had a larger soma and a more depolarised resting membrane potential, a lower spike-threshold, and longer-lasting AHPs (Table 1, left-hand columns). In addition, they showed repetitive firing at apparently irregular spike intervals in response to supra-threshold stimuli (Figure 1b; Kawaguchi, 1992). A burst-like firing pattern or plateau-like persistent depolarisation spikes, typical features of parvalbumin or somatostatin containing neostriatal GABAergic interneurones (Kawaguchi, 1993; Kawaguchi *et al.*, 1995; Plenz & Kitai, 1998), respectively, was never observed.

These data indicate that the recordings were made exclusively from medium-spiny neurones and cholinergic interneurones, a suggestion in accordance with the abundance of MS cells in the caudate–putamen (>90% of the neuronal population; Kawaguchi *et al.*, 1995) and with our effort to record also from large diameter neurones, an approach which certainly has favoured the percentage of LA cells in the population recorded from.

Electrophysiology: P2X receptors

After the electrophysiological characterisation of neurones had been accomplished, currents induced by pressure application of the $GABA_A$ receptor agonist muscimol (10 μM) and the P2X receptor agonists ATP (100–1000 μM), 2MeSATP and α,βmeATP (30–300 μM, each) were measured under voltage-clamp conditions at the holding potential of −80 mV in the same set of cells. Under these conditions, pressure application of ACSF without added receptor agonist did not evoke detectable membrane currents, neither in MS cells ($n=5$) nor

Table 1 Properties of medium-spiny projection neurones (MS cells) and cholinergic interneurones (LA cells) in the rat caudate–putamen (neostriatum)

	Present study		*Data from literature*[a]	
	MS cells (n=82)	*LA cells (n=54)*	*MS cells*	*LA cells*
Soma diameter (μm)	17.2±0.5	33.9±1.8*	12–25	20–61
Resting potential (mV)	−86.2±0.9	−65.0±1.6*	∼−80	∼−60
Spike threshold (mV)	42.3±1.9	18.3±1.6*	∼44	∼17
Time to peak of AHP (ms)	21.2±1.8	36.7±3.5*	∼20	∼50

[a]References: Kawaguchi (1992); Kawaguchi (1993); Kawaguchi *et al.* (1995); Plenz & Kitai (1998).
*$P<0.05$, significant differences from MS cells. AHP = after-hyperpolarisation; LA = long-lasting after-hyperpolarisation; MS = medium spiny. The greater somatic diameter was measured from neurones visualised under DIC optics. All other parameters were measured under current clamp conditions. The spike threshold was the voltage difference between the resting potential and the onset of the first action potential elicited in response to a series of stepwise (10 pA) increasing depolarising current pulses. The time to peak of AHP was the time difference between spike onset and the voltage peak of the AHP.

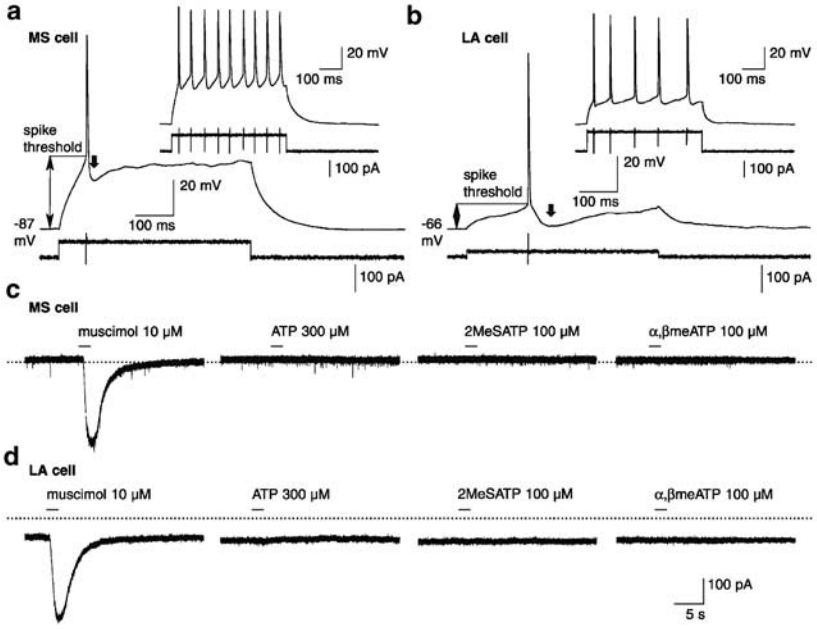

Figure 1 Electrophysiological characterisation (a, b) and agonist-induced transmembrane currents (c, d) obtained in a medium-spiny neurone (a, c; MS cell) and a cholinergic interneurone (b, d; LA cell) contained in rat neostriatal brain slices. Action potentials and membrane currents were recorded under current-clamp and voltage-clamp conditions, respectively. (a, b) Representative action potential patterns (upper panels) of an MS cell and an LA cell, respectively, evoked by just-threshold 500 ms depolarising current pulses (lower panels). The insets in (a, b) show action potential patterns (upper panels) of the respective cells evoked by supra-threshold current injection (lower panels). The MS cell differed from the LA cell by its higher spike threshold and shorter time to the peak of AHP (arrows) in response to the just-threshold stimulus. Upon supra-threshold stimulation, the MS cell fired at evenly spaced spike intervals, whereas the spike discharge of the LA cell showed accommodation. (c, d), only the $GABA_A$ receptor agonist muscimol (10 μM) but not the P2X receptor agonists ATP (300 μM), 2MeSATP and α,βmeATP (100 μM, each) elicited inward currents (downward deflections) in the MS cell and the LA cell, respectively. Agonists were subsequently applied for 2 s each. Between pressure applications, cells were superfused with drug-free ACSF for 2 min. In this and subsequent figures, the dotted lines indicate the zero current level and the horizontal bars above the current traces the times of agonist application.

LA cells ($n=5$). In the greater proportion of experiments, the sequence of agonist application was muscimol–ATP–2MeSATP–α,βmeATP. However, when this order was varied results were similar and, hence, were pooled (see also legend to Table 2). Responses of a representative MS cell and a representative LA cell recorded under control conditions are shown in Figure 1c and d. The statistical evaluation of a greater number of MS and LA cells is given in Table 2 (Control). Obviously, ATP and its two structural analogues failed to cause any detectable transmembrane current. Muscimol, in contrast, evoked inward currents in the MS cells, as well as LA cells. Both, ATP and 2MeSATP can be rapidly degraded by ectoATPases, whereas α,βmeATP is relatively resistant to these enzymes (Welford *et al*., 1987). The latter compound, however, possesses only negligible activity at homomultimeric $P2X_2$ (Brake *et al*., 1994) and $P2X_4$ receptors (Bo *et al*., 1995), which may be present in the striatum (Lê *et al*., 1998; Kanjhan *et al*., 1999). Therefore, the likewise hydrolysis-resistant ATP analogue ATPγS (Welford *et al*., 1987), which actually had considerable activity at these receptors (see Methods), was added in some experiments to the sequence of pressure applied P2X receptor agonists. However, ATPγS (100 μM) did not evoke measurable inward membrane current responses, neither in MS cells (2.1 ± 4.3 pA; $n=7$) nor in LA cells (0 ± 5.3 pA; $n=4$).

Nevertheless, ecto-enzymes may have produced some adenosine from the P2X agonists in the brain slices. In order to prevent possible opposing actions of adenosine at coexisting adenosine A_1 receptors (Tschöpl *et al*., 1992), the second series of experiments in electrophysiologically characterised MS and LA neurones was carried out in the presence of the preferential A_1 adenosine receptor antagonist DPCPX (Fredholm *et al*., 1994; 0.1 μM). However, the adenine nucleotides again failed to induce membrane current responses, whereas muscimol evoked the usual inward currents (Table 2, DPCPX).

In a third series of experiments, brain slices were incubated for a 1–6 h period in ACSF also containing the ATP–ADPase apyrase (10 U ml^{-1}), an attempt to recover P2X receptor activity from a possible desensitisation by endogenous ATP (Buell *et al*., 1996). Before recordings were initiated, slices were kept for an additional 15–30 min equilibrium period in apyrase-free ACSF. However, ATP, 2MeSATP and α,βmeATP did not evoke P2X receptor-mediated transmembrane currents under these conditions, neither in MS neurones nor in LA neurones (Table 2, Apyrase). Muscimol-induced inward currents were much smaller in amplitude than those observed in the absence of apyrase (compare Table 2, Control). Possibly, the enzyme could have competed with an ecto-protein kinase for endogenous ATP. Such ecto-kinases have been suggested to increase NMDA receptor activity in hippocampal neurones (Fujii *et al*., 2002), and could also, in analogy enhance $GABA_A$ receptor activity in the neostriatal neurones.

Table 2 Effects of the $GABA_A$ receptor agonist muscimol and of the P2 receptor agonists ATP, 2MeSATP and α,βmeATP in medium-spiny neurones (MS cells) and cholinergic interneurones (LA cells) in the rat caudate–putamen

	Transmembrane current (pA)									
	Muscimol (μM)	*ATP (μM)*			*2MeSATP (μM)*			*α,βmeATP (μM)*		
	10	*100*	*300*	*1000*	*30*	*100*	*300*	*30*	*100*	*300*
Control										
MS cells ($n=9$)	−210.6±52.9*	−5.5±4.6			−6.3±4.0			3.6±4.5		
LA cells ($n=4$)	−222.5±84.4*	2.5±7.2			−2.5±4.6			−4.5±3.8		
MS cells ($n=48$)	−256.6±54.4*		1.2±2.9			1.1±2.7			3.1±3.6	
LA cells ($n=34$)	−252.9±44.9*		1.9±1.3			1.3±0.8			2.3±2.8	
MS cells ($n=9$)	−231.6±37.4*			−0.1±3.7			4.6±3.5			4.4±3.3
LA cells ($n=4$)	−266.9±123.6*			3.0±6.3			6.8±5.4			−1.5±4.0
DPCPX (0.1 μM)										
MS cells ($n=5$)	−212.0±65.8*		4.2±2.3			0.4±0.4			3.9±1.6	
LA cells ($n=4$)	−207.0±101.8*		−0.5±2.5			0.5±2.9			1.8±1.2	
Apyrase (10 U ml^{-1})										
MS cells ($n=4$)	−88.8±21.3*		−5.5±8.6			−1.5±4.2			−4.5±3.1	
LA cells ($n=3$)	−47.0±14.1*		−0.7±1.8			1.7±1.7			3.7±1.9	
CsCl pipette										
MS-like cells ($n=4$)	−619.0±128.8*		2.3±2.3			3.0±2.1			7.3±4.4	
LA-like cells ($n=3$)	−950.0±101.9*		0.3±0.3			6.0±6.0			1.7±1.7	

*$P<0.05$, significant differences from zero. Inward currents negative in sign. Data are peak current amplitudes in response to the respective agonists. Muscimol, ATP and its structural analogues were consecutively pressure applied (2 s) to the same neurone. Between the individual applications, cells were superfused with drug-free ACSF for 2 min. In most experiments, the sequence of agonist application was, as given in the table, muscimol (10 μM)–ATP (300 μM)–2MeSATP (100 μM)–α,βmeATP (100 μM). In experiments where the higher or lower concentrations of P2X receptor agonists were tested, the order of agonist application was intermingled or reversed. In the apyrase experiments, brain slices were stored in ACSF containing the enzyme at least for 1–6 h prior to the start of recordings. In experiments with DPCPX, the adenosine receptor antagonist was added to the ACSF at least 15 min prior to the recordings and for the remainder of the experiments. CsCl (140 mM) replaced K-gluconate in the pipette solution. Control, experiments carried out in the absence of apyrase or DPCPX with the K-gluconate pipette solution.

Since ATP had activated *via* P2Y receptors potassium outward currents in cultured striatal neurones (Ikeuchi & Nishizaki, 1995), which, if present, could have opposed P2X receptor-mediated inward currents in our experiments, the fourth series of experiments, aimed to detect functional P2X receptors in neostriatal neurones, was carried out when K^+ channels were blocked by means of a CsCl-based intracellular solution. Under these conditions, an electrophysiological characterisation of the investigated cells was no longer possible and the classification had to relay solely on morphological criteria. However, judged from the experiments documented in the preceding section, four cells having a greater somatic diameter of 13.0±0.6 μM and three cells having a greater somatic diameter of 27.3±0.7 μM were most likely MS neurones and LA neurones, respectively. ATP, 2MeSATP and α,βmeATP did not induce transmembrane currents under these conditions (Table 2, CsCl). Muscimol-induced currents were larger in amplitude when measured with the CsCl instead of the usual K-gluconate internal solution (compare Table 2, Control). This may be explained by the greater driving force for Cl^- through open $GABA_A$ receptor channels at the holding potential of −80 mV, because the Cl^- equilibrium potential shifted from −62 (K-gluconate) to 3 mV (CsCl). ATP and its structural analogues were also ineffective in six presumptive MS cells and two presumptive LA cells when the intracellular CsCl solution was combined with extracellular DPCPX (0.1 μM; data not shown).

Eventually, the question may arise, whether the experimental design, used in the trials mentioned so far, was at all adequate to detect P2X receptor-mediated currents in brain slice preparations. Since LC neurones are known to posses functional P2X receptors (Tschöpl *et al*., 1992; Shen & North, 1993), and, additionally, the presence of $P2X_1$–$P2X_6$ proteins has been proven there (Yao *et al*., 2000), we used an LC brain slice preparation as control.

In order to unambiguously identify the LC neurones, a single test concentration (100 μM) of noradrenaline was pressure applied, at the beginning of each experiment, in the cell-attached patch-clamp configuration. It produced a complete and reversible inhibition of spontaneous action potential discharge (Figure 2Aa), a distinctive feature for these neurones (e.g. Nörenberg *et al*., 1997a).

After gaining whole-cell access, muscimol (10 μM), ATP (300 μM), 2MeSATP (100 μM) and α,βmeATP (100 μM) were consecutively pressure applied to the same set of neurones. The sequence of agonists was varied between the experiments. The $GABA_A$ receptor agonist muscimol (−209.3±45.8 pA), as well as the P2X receptor agonists ATP (−71.4±11.0 pA) and 2MeSATP (−77.5±14.6 pA) evoked inward currents at the holding potential of –80 mV in all LC neurones tested ($n=9$–11; Figure 2Ab, B). The ATP analogue α,βmeATP (100 μM) was ineffective in five neurones (exemplified in Figure 2Ab). In the remaining five LC cells, it evoked an inward current of −21.0±12.6 pA (Figure 2B). While it has been already reported that α,βmeATP was less potent at P2X receptors in the LC than ATP and 2MeSATP (see Methods; Shen & North, 1993), we have, at the present, no clear explanation for its lack of effect in a proportion of neurones. A suggestive reason,

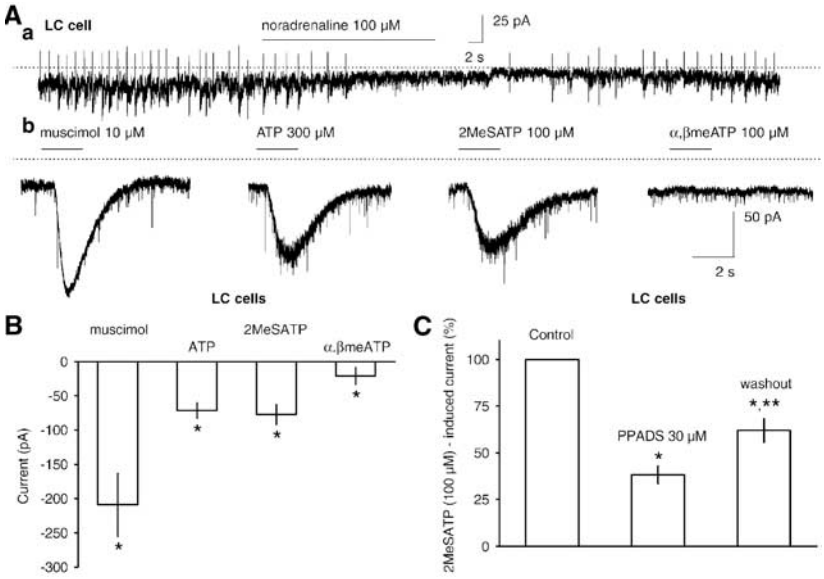

Figure 2 Electrophysiological characterisation (Aa), agonist-induced transmembrane currents (Ab, B) and antagonism by PPADS of 2MeSATP-induced transmembrane currents (C) in noradrenergic locus coeruleus (LC) neurones contained in rat pontine brain slices. The holding potential was −80 mV. (Aa) Cell-attached recording showing the reversible inhibition of extracellularly recorded spontaneous action potential firing (fast vertical deflections) in an LC neurone by pressure application (25 s) of noradrenaline (100 μM). (Ab) Same cell as in (Aa) after the cell membrane was ruptured to gain whole-cell access. Inward currents evoked by pressure application of the $GABA_A$ receptor agonist muscimol (10 μM), as well as the P2X receptor agonists ATP (300 μM), 2MeSATP and α,βmeATP (100 μM, each) are shown. Is is to be noted that α,βmeATP did not evoke an inward current in this cell. Agonists were subsequently applied for 2 s each. Between pressure applications, cells were superfused with drug-free ACSF for 2 min. (**B**) Means ± s.e.m. of inward currents obtained under the conditions of (Ab) are shown; $*P<0.05$, significant differences from zero; ($n=9$–11). (**C**) Interaction between 2MeSATP (100 μM) and PPADS (30 μM). 2MeSATP was pressure applied three times to the same set of neurones with 10 min interval. PPADS was present in the bath for 10 min before and during the second application of 2MeSATP. Inward currents expressed as percentage of current amplitudes obtained before superfusion with PPADS (Control) are shown. $*P<0.05$, significant difference from Control; $**P<0.05$, significant difference from currents obtained in the presence of PPADS ($n=3$).

strong P2X receptor desensitisation during repetitive agonist exposures, was not likely to fully account for this. The compound was also ineffective when applied as the first in the series of agonists ($n=2$), and furthermore, P2X receptor-mediated effects in LC neurones showed, if at all (Tschöpl *et al*., 1992), only little desensitisation (Shen & North, 1993). Remarkably however, not all cells in the LC seemed to express $P2X_1$ and $P2X_3$ (Yao *et al*., 2000), subunits which can confer α,βmeATP sensitivity to homomultimeric, as well as heteromultimeric P2X receptors (North, 2002).

The P2X receptor antagonist pyridoxalphosphate-6-azophenyl-2′,4′-disulphonic acid (PPADS 30 μM; Lambrecht *et al*., 1992) inhibited 2MeSATP (100 μM)-induced inward currents by 61.9 ± 4.8%, an effect, in accordance with its known slow dissociation from P2X receptors (Li, 2000), only partially but significantly reversible during a 10 min period of washout ($n=3$, Figure 2C).

The results obtained in the LC neurones, however, did not exclude the existence of diffusion barriers, being present in the neostriatum and not in the LC, which may have prevented the access of ATP and its analogues to P2X receptors but not that of muscimol to $GABA_A$ receptors. Accordingly, we found that the times to agonist equilibrium at the $GABA_A$ receptors, when estimated by measuring the rise times from 10 to 90% of the peak muscimol-induced currents, were similar in LC neurones (1276 ± 197 ms; $n=6$) and neostriatal neurones (1126 ± 86 ms; $n=10$; $P>0.05$). In the last series of experiments aimed to detect functional P2X receptors in neurones from the caudate–putamen, we therefore took advantage of the nucleated outside-out configuration of the patch-clamp technique (Sather *et al*., 1992). This technique allowed us, after neurones had been characterised beforehand either as MS cells or LA cells during conventional whole-cell recordings, to withdraw from the cells under investigation the patch pipettes together with large outside-out membrane vesicles. These vesicles could then be lifted several 10th of micrometers above the brain slice surface, a situation where the diffusion of agonists to their receptors should be greatly improved.

Muscimol (10 μM) evoked inward currents in all patches excised from MS cells (Figure 3a, c) and all LA cells (Figure 3b, d), with average peak amplitudes of –66.8 ± 18.1 ($n=7$) and −69.5 ± 17.0 pA ($n=5$), respectively. According to our expectations, we found that the 10–90% rise times of the muscimol-induced currents (201 ± 20 ms; $n=12$; $P<0.05$) were now significantly shorter than in neostriatal neurones or LC neurones contained in the slice preparations, indicating indeed a facilitated diffusion of the agonist to its receptors.

The effect of muscimol was greater in intact cells than in the excised patches (compare Table 2, Control). However, taking into account the different surface areas (calculated from the capacitance settings of the patch-clamp amplifier by assuming a specific membrane capacitance of 1 μF/cm^2) of roughly 1459 ± 128, 2700 ± 379 and 197 ± 14 μM^2 for MS cells, LA cells and nucleated outside-out patches ($n=12$, each), respectively, the difference may be explained by the greater number of

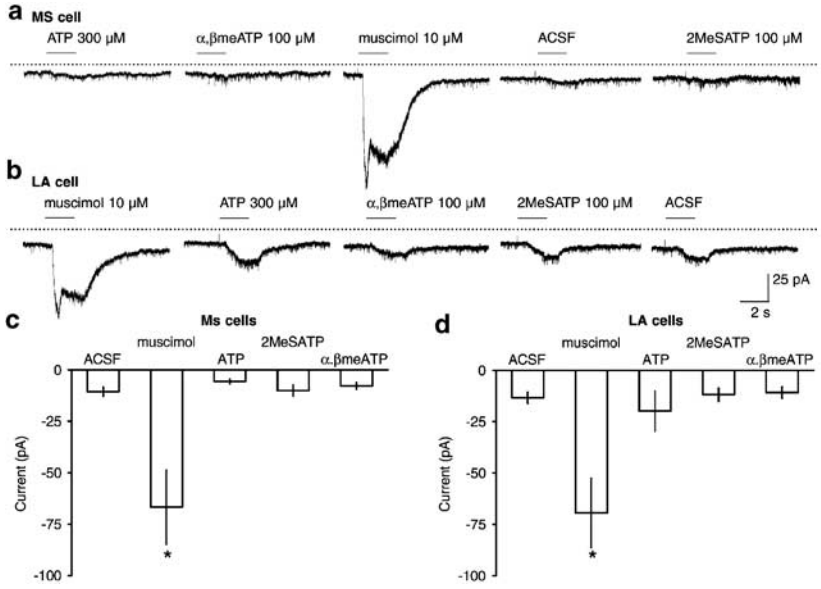

Figure 3 Agonist-induced transmembrane currents obtained in nucleated outside-out patches excised from medium-spiny neurones (a, c; MS cell) and cholinergic interneurones (b, d; LA cell) contained in rat neostriatal brain slices. After neurones had been electrophysiologically characterised either as MS cells or LA cells (see Figure 1, Table 1) under current-clamp in the whole-cell configuration of the patch-clamp technique, nucleated outside-out patches were constructed by carefully withdrawing patch pipettes from the cells while maintaining light suction to the pipette interior during the period of withdrawal. Subsequently, the patch pipettes were lifted together with the adherent outside-out membrane vesicles above the brain slice surface, an attempt to circumvent diffusion barriers presumably present within the slice tissue. (a, b) Representative inward currents evoked at the holding potential of -80 mV by pressure application of bath solution (ACSF), or bath solution containing also the $GABA_A$ receptor agonist muscimol (10 μM), as well as the P2X receptor agonists ATP (300 μM), 2MeSATP and α,βmeATP (100 μM, each) in nucleated outside-out patches excised from an MS cell (a) and an LA cell (b), respectively. Agonists (or ACSF alone) were subsequently applied for 2 s each. Between pressure applications, cells were superfused with drug-free ACSF for 2 min. (c, d) Means $\pm$ s.e.m. of inward currents obtained under the conditions of (a, b) in nucleated outside-out patches from MS cells (c; $n=7$) and LA cells (d; $n=5$). *$P<0.05$, significant differences from currents evoked by pressure application of ACSF alone.

$GABA_A$ receptor channels available in the larger membrane area of the intact cells.

The muscimol-induced currents in nucleated outside-out patches from MS cells and LA cells (Figure 3a, b) displayed also kinetics different from the currents obtained in conventional whole-cell recordings (compare Figure 1c, d; Figure 2Ab). They were characterised by a rapid rising phase followed by a rapid decay and then by a slow and pronounced rebound. We have not investigated further the reason for this. However, under conditions of ultrafast agonist application, a similar kinetic behaviour was already described for GABA-induced currents in outside-out patches from cultured hippocampal neurones, where the fast decaying phase of the current was attributed to a self-block of the channel pore by the agonist, whereas the rebound phase may reflect the reactivation of $GABA_A$ receptors from the desensitised conformation during prolonged agonist application (Mercik *et al*., 2002).

ATP (300 μM), 2MeSATP and α,βmeATP (100 μM, each) elicited also tiny inward currents in the nucleated outside-out patches withdrawn from MS cells (Figure 3a, c) and LA cells (Figure 3b, d). Thus, current amplitudes induced by for example, ATP were -5.7 ± 1.2 and -19.9 ± 9.9 pA in seven patches from MS cells and five patches from LA cells, respectively. These were, however, not P2X receptor-mediated currents because they did not significantly differ from currents evoked by pressure application of bath solution (ACSF) with no added ATP (MS cells: -10.7 ± 2.3 pA; LA cells: -13.4 ± 2.7 pA; $P>0.05$). The same was true for the currents elicited by 2MeSATP and α,βmeATP. The muscimol-induced currents, however, were significantly greater than currents evoked by ACSF alone (Figure 3c, d).

We did not further characterise the mechanisms underlying the small currents evoked by pressure application of bath solution. However, one may speculate that they possibly were carried through mechanosensitive channels, the activation of which might have been facilitated by membrane stress during the nucleated outside-out patch fabrication (Wan *et al*., 1999).

Taken together so far, the results from 92 MS cells or MS-like cells and 59 LA cells or LA-like cells indicated that functional soma-dendritic P2X receptors were absent from medium-spiny projection neurones and cholinergic interneurones, respectively, in the caudate–putamen from 5–26-day-old rats. They corroborate, however, the presence of functional P2X receptors in noradrenergic neurones from the rat LC.

Electrophysiology: P2Y receptors

To reveal a possible P2Y receptor-mediated activation of K^+ channels (Ikeuchi & Nishizaki, 1995), ATP (100 μM) was also pressure-applied to the neostriatal neurones for 30 s instead of the usual 2 s. Even after this prolonged application period, no change in holding current in response to ATP was detected ($n=14$), an observation corroborating the absence of functional P2X receptors.

In order to detect any ATP-induced change in membrane conductance, ramp depolarisations (-140 to $+40$ mV at

$0.18\,mV\,s^{-1}$) were imposed two times to neurones voltage-clamped at a holding potential of $-80\,mV$, first in the absence of ATP ($100\,\mu M$; see Methods) and, second, after 30 s of pressure application in the continued presence of the nucleotide. In these experiments, voltage-dependent Na^+ channels were blocked by TTX ($0.3\,\mu M$) to avoid voltage-clamp problems caused by the activation of uncontrollable large Na^+ currents. Of course, TTX prevented the classification of neurones on the basis of their firing pattern. However, cells having a greater somatic diameter of $17.5\pm1.0\,\mu M$ and a resting membrane potential of $-79.6\pm2.7\,mV$ ($n=12$) were most likely MS neurones, whereas two cells having a greater somatic diameter of 24 and $29\,\mu M$ and a resting membrane potential of -50 and $-59\,mV$ were most likely LA neurones (compare Table 1).

Representative recordings from such provisionally characterised MS cells and LA cells are shown in Figure 4a and b, respectively. ATP ($100\,\mu M$) had no effect on the membrane conductance in the 12 MS-like and two LA-like cells: currents evoked by the voltage ramps in the absence or in the presence of ATP were superimposed. When ADP ($100\,\mu M$; see Methods), which is in contrast to ATP a full agonist at least at human $P2Y_1$ (von Kügelgen & Wetter, 2000), was used in another seven MS-like and two LA-like cells, the results were comparable. ADP was also ineffective after pretreatment (1–6 h) of the brain slices with $10\,U\,ml^{-1}$ of apyrase ($n=7$ and 4, MS-like and LA-like cells, respectively; data not shown).

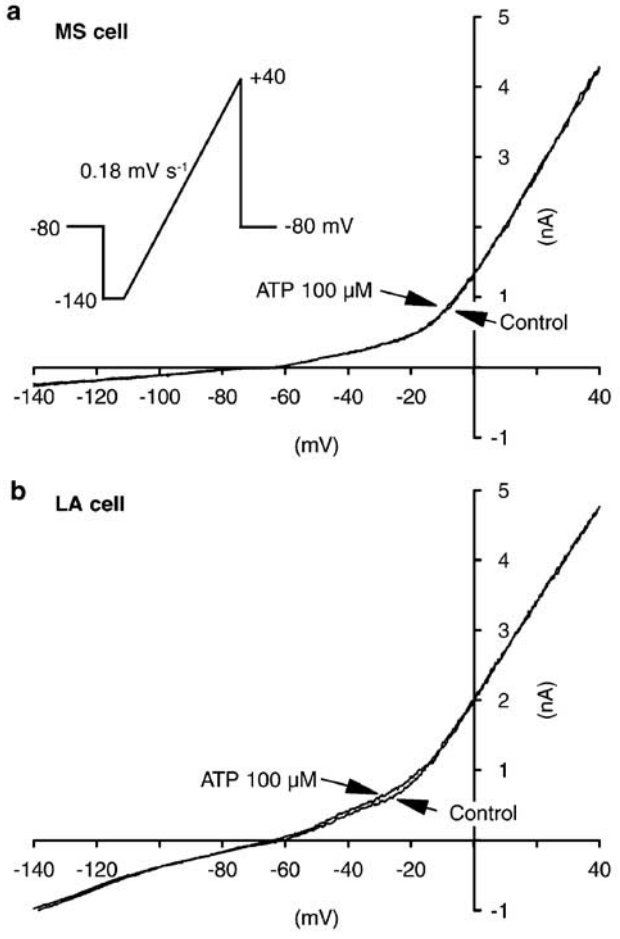

Figure 4 Representative current–voltage relationships obtained from a presumptive medium-spiny projection neurone (a; MS cell) and a presumptive cholinergic interneurone (b; LA cell) in rat neostriatal brain slices. The current–voltage relationships were constructed from membrane current responses to voltage ramps (-140 to $+40\,mV$ at $0.18\,m\,s^{-1}$; inset in a), imposed from a holding potential of $-80\,mV$, first in the absence and, then after 30 s in the continued presence of ATP ($100\,\mu M$). TTX ($0.3\,\mu M$) was present in the ACSF. It is to be noted that the currents obtained in the absence (Control) and presence of ATP were essentially identical.

Immunocytochemistry and confocal microscopy

To scrutinise the obvious discrepancy between the evidence from literature for the presence of at least $P2X_2$, $P2X_4$ and $P2Y_1$ in neostriatal neurones (Lê *et al*., 1998; Kanjhan *et al*., 1999; Moore *et al*., 2000; Franke *et al*., 2003) and the lack of receptor activity (present study), we next asked whether the cells in which electrophysiological recordings were successful, might have represented a biased population devoid of such receptor proteins.

To this end, a proportion of neostriatal neurones was filled with the fluorescent dye LY during the electrophysiological recordings, in order to allow their recovery for subsequent immunostaining with specific antibodies directed against $P2X_2$, $P2X_4$ or $P2Y_1$ receptor proteins. A total of 15 cells were characterised as belonging to either the MS class ($n=6$) or the LA class ($n=9$), respectively, by the criteria illustrated in Table 1 and Figure 1. Muscimol evoked in these cells the usual inward currents, whereas ATP, 2MeSATP and α,βmeATP lacked any effect (Table 2, Control). The remainder of the LY-filled cells were tentatively assigned to either the MS class ($n=10$) or the LA class ($n=5$), based on measurements of their somatic diameter, as well as resting membrane potential, in experiments where ADP lacked any effect on the membrane conductance (preceding section and Figure 4).

The intracellular filling with LY resulted in a clear fluorescence signal of the studied MS and LA cells as shown in the confocal photomicrographs of Figure 5 (LY; a, d, g, j, m, p). Three out of five MS neurones and two out of five LA neurones showed $P2X_2$ immunofluorescence (IF) after staining with the respective Cy3-coupled antibody (Figure 5b, k). This IF was confined to the perikarya and colocalised with the LY-autofluorescence (Figure 5c, l). The overall level of $P2X_2$-IF in the neostriatal slices seemed to be low: $P2X_2$-positive perikarya adjacent to the LY-filled cells were infrequent (e.g. Figure 5b and k). Nevertheless, $P2X_2$-positive fibres, which did not colocalise with the LY-autofluorescence (arrows in Figure 5b and c), were occasionally observed.

$P2X_4$ antibodies did not colocalise with LY in the samples of MS cells ($n=4$; Figure 5d–f) or LA cells ($n=6$; Figure 5m–o) used for electrophysiology but isolated $P2X_4$-positive fibres were sometimes seen (arrows in Figure 5e, f).

Four out of seven MS neurones and two out of three LA neurones showed $P2Y_1$-IF after staining with the respective Cy3-coupled antibody (Figure 5h, q). The combination of

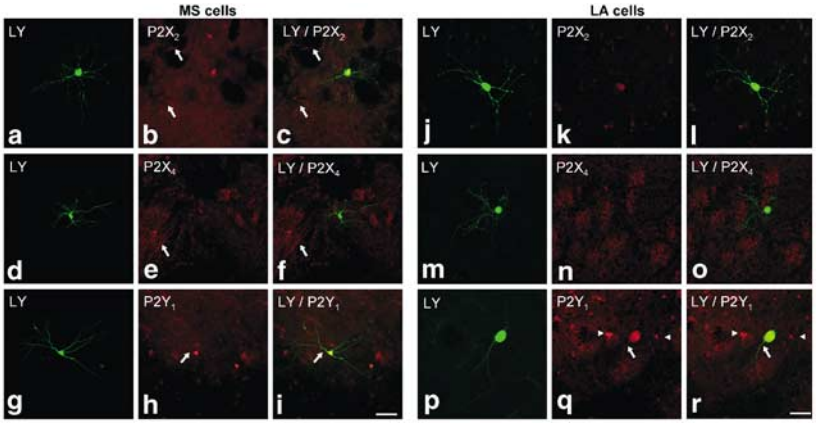

Figure 5 Confocal microscopy images from rat neostriatal medium-spiny projection neurones (MS cells, a–i) and cholinergic interneurones (LA cells, j–r) obtained in rat neostriatal brain slices showing yellow–green Lucifer yellow (LY) autofluorescence (a, d, g, j, m, p), red Cy3 immunofluorescence for $P2X_2$ (b, k), $P2X_4$ (e, n) and $P2Y_1$ receptors (h, q), as well as the colocalisation of LY and P2 receptor–Cy3-fluorescence (c, f, i, l, o, r). Neurones were intracellularly perfused with an LY (1.5%) containing pipette solution during whole-cell recordings and displayed electrophysiological properties typical for MS cells or LA cells. After recordings had finished, slices were fixed and incubated with the respective P2 receptor-specific antibodies. Primary antisera were localised by the secondary Cy3-coupled antibody. The arrows in (b, c and e, f) indicate isolated $P2X_2$- and $P2X_4$-positive fibres, respectively. The arrows in (h, i and q, r) indicate $P2Y_1$-positive proximal process of the LY-filled cells. The arrowheads in (q, r) indicate $P2Y_1$-positive perikarya adjacent to the LY-filled cell. Scale bars: 50 μM.

LY-autofluorescence with $P2Y_1$-IF revealed a clear colocalisation (Figure 5i, r). The $P2Y_1$-IF was observed on the cell bodies and on the proximal processes (arrows in Figure 5h, i, q, r). Overall, the level of $P2Y_1$-staining appeared higher when compared to the $P2X_2$-staining: $P2Y_1$-IF-positive perikarya were frequently observed in the neighbourhood of the LY-filled cells (e.g. arrowheads in Figure 5q, r).

So far, the immunohistochemical data indicate that roughly half of the rat neostriatal neurones used for electrophysiological recordings, medium-spiny projection neurones, as well as cholinergic interneurones expressed $P2X_2$- and $P2Y_1$ receptor proteins despite the apparent lack of corresponding receptor activity.

The above experiments, however, did not definitively exclude the possibility that the observed $P2X_2$ (and $P2Y_1$) protein labelling was somehow artefactually introduced, for example, by filling cells with LY. Therefore, we performed additional P2 receptor immunostaining experiments in tissues not subjected to electrophysiological recordings that were fixed by transcardial perfusion of the animals prior to the fabrication of the neostriatal brain slices.

Representative results ($n = 3$ animals) are shown in Figure 6. Neuronal cells within the neostriatal brain sections were identified by a mouse antibody against the differentiated neurone-specific MAP2 (Izant & McIntosh, 1980). No further attempts were made to classify these cells into the known striatal neuronal subtypes. The localisation of anti-MAP2 with a Cy2-conjugated goat anti-mouse IgG resulted in clear fluorescence signals from neuronal perikarya and processes (Figure 6a, d, g). MAP2-positive neuronal cells showed colocalisation with $P2X_2$ (Figure 6b, c), P2X4 (Figure 6e, f) and P2Y1-IF (Figure 6h, i).

Taken together, the immunohistochemical data corroborate the existence of $P2X_2$, $P2X_4$ and $P2Y_1$ receptor proteins in rat neostriatal neurones. Regarding the preponderance of medium spiny neurones in the caudate–putamen, it is most likely that at least some of the P2 receptor-positive neuronal cells found in sections from perfused rats were of this class. Hence, it seems implausible that the $P2X_2$- and $P2Y_1$-IF seen in electrophysiologically identified medium-spiny neurones, as well as cholinergic interneurones, were artefacts caused by experimental interventions. The nature of the $P2X_4$-positive cells remained somewhat more obscure although it has been proposed on grounds of morphological criteria that these were also medium-spiny cells (Lê *et al*., 1998).

Discussion

As a whole, the present results strongly suggest that neostriatal medium-spiny neurones and cholinergic interneurones can synthesise P2X ($P2X_2$ and possibly $P2X_4$) and P2Y ($P2Y_1$) receptor proteins. Moreover, they also indicate that at least $P2X_2$ and $P2Y_1$ were present in a proportion of cells used for electrophysiology. In so far as soma-dendritic receptors were concerned, the $P2X_2$ (and possibly $P2X_4$) subunits were not functional. Whether the $P2Y_1$-IF indicated the presence of functional G protein-coupled receptors remained unclear. That is because the data from the present study cannot exclude the possibility that the $P2Y_1$ immunofluorescence had represented functional receptors primarily not implicated in transmembrane current generation. Be that as it may, fundamental differences between cultured neostriatal neurones, where ATP-sensitive P2Y receptors mediated the activation of K^+ channels (Ikeuchi & Nishizaki, 1995), and neurones contained in neostriatal brain slices seem to exist.

At present, we have no clear mechanistic resolution for the striking inconsistency between the presence of P2X receptor proteins in a fraction of neostriatal neurones and the apparent lack of respective function. The most parsimonious explanation is that the $P2X_2$ (and possibly $P2X_4$)IF did not represent membrane-bound ATP-gated receptor channels.

Improperly folded or assembled ionotropic receptors cannot exit the endoplasmic reticulum (ER; Deutsch, 2003). This was

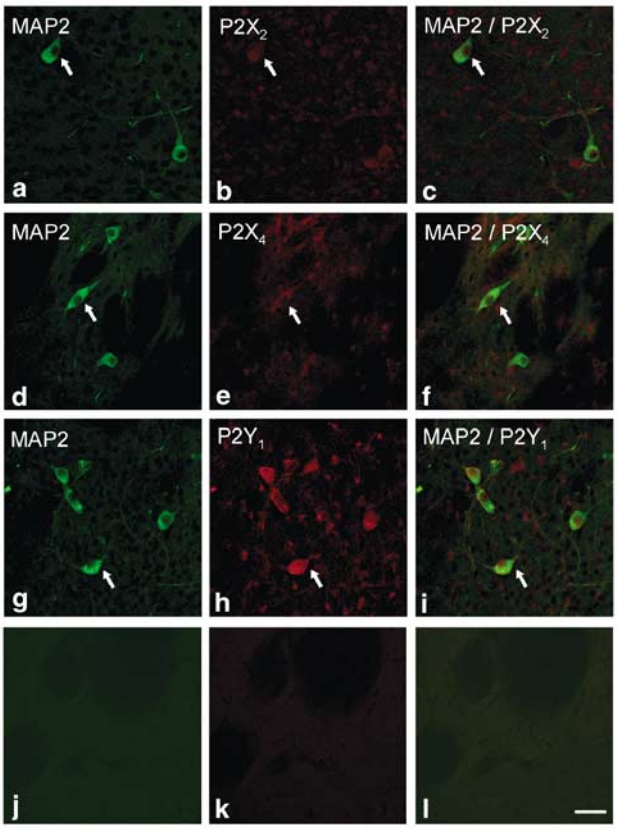

Figure 6 Confocal microscopy images from MAP2-positive neurones in neostriatal brain slices from transcardially perfused rats. The yellow–green neuronal microtubule associated protein (MAP2)–Cy2 immunofluorescence (IF; a, d, g), the red Cy3-IF for $P2X_2$ (b), $P2X_4$ (e) and $P2Y_1$ receptors (h), as well as the colocalisation of MAP2–CY2-IF with the P2 receptor–Cy3-IF (c, f, i,) are shown. (j–l) Representative examples for the unspecific background labelling obtained by Cy2 (j), Cy3 (k) and the combination of Cy2 with Cy3 (l) when the primary MAP2 and P2 receptor antibodies were omitted from the staining protocol. Please note that identifiable cellular striatal components were not stained under these conditions. Anaesthetised rats were perfused transcardially with paraformaldehyde and glutaraldehyde. After decapitation, brain slices were incubated in a mixture of MAP2- and the respective P2 receptor-specific antibodies. Primary antisera were localised by the secondary Cy2- (MAP2) and Cy3-coupled antibodies (P2 receptors). Arrows indicate examples of P2 receptor–MAP2-colocalisation. Scale bar: 50 μM.

shown, for example, for the NR3A subunit of the NMDA receptor family, which was retained there unless coexpressed and coassembled with NR1 (Pérez-Otaño *et al*., 2001). The same may be true for P2X proteins. Concatenated $P2X_1$ subunits, even in the trimeric conformation assumed for native receptors, formed large aggregates in the ER and occurred in only small amounts as functional receptors in the plasma membrane (Nicke *et al*., 2003). From that, it was suggested that hetero-oligomerisation with other P2X subtypes could impose a differentially folded conformation on the receptor complex, capable of better passing the ER quality control system (Nicke *et al*., 2003). Hence, it seems conceivable that the P2X receptor subunits in the neostriatal neurones may not be transported to the cell membrane. That $P2X_2$ and $P2X_4$ did not hetero-oligomerise with each other (Torres *et al*., 1999) may thus support this notion. Alternatively, the receptors may not be stabilised in the plasma membrane. Particularly, $P2X_4$ receptors showed, due to the existence of a C-terminal endocytic motif, a high rate of constitutive internalisation (Royle *et al*., 2002), and the bulk of striatal $P2X_4$-IF was indeed found to be localised intracellularly (Lê *et al*., 1998).

Eventually, one should remind that P2X receptor expression can be dynamically regulated. In, for example,neurones from LC and spinal cord, P2X receptor activity increased during development (Wirkner *et al*., 1998; Jang *et al*., 2001) and, moreover, in the hippocampus, $P2X_2$ and $P2X_4$ proteins were upregulated following ischemia (Cavaliere *et al*., 2003). Therefore, the present data do not exclude that the pre-existing $P2X_2$ (and possibly $P2X_4$) subunits in the neostriatal neurones may become functional under certain, however, yet unknown conditions. $P2X_2$ and $P2X_4$ subunits hetero-oligomerise with $P2X_6$ (Torres *et al*., 1999) and $P2X_6$ mRNA was detected in the striatum (Collo *et al*., 1996). Hence, it is tempting to speculate, supposed hetero-oligomerisation would indeed facilitate the trafficking of P2X receptors, that any signal inducing the upregulation of $P2X_6$, which on its own did not readily assemble into functional homomultimeric ATP-gated channels (Collo *et al*., 1996), may concomitantly aid the membrane targeting of the otherwise silent $P2X_2$ and $P2X_4$ subunits.

We are grateful to M. Henschke for technical assistance and Dr J. Grosche (Department of Neurophysiology, Paul-Flechsig-Institute of Brain Research, University of Leipzig) for the confocal laser scanning microscopy. This study was supported by the 'Deutsche Forschungsgemeinschaft' (IL 20/9-2), the 'Bundesministerium für Bildung, Forschung und Technologie' (Deutsch – Polnische Zusammenarbeit in den Neurowissenschaften) and the Interdisciplinary Centre for Clinical Research at the University of Leipzig (01KS9504, Project C14, Z10).

References

ABBRACCHIO, M.P., BOEYNAEMS, J.M., BARNARD, E.A., BOYER, J.L., KENNEDY, C., MIRAS-PORTUGAL, M.T., KING, B.F., GACHET, C., JACOBSON, K.A., WEISMAN, G.A. & BURNSTOCK, G. (2003). Characterization of the UDP-glucose receptor (re-named here the $P2Y_{14}$ receptor) adds diversity to the P2Y receptor family. *Trends Pharmacol. Sci.,* **24,** 52–55.

BO, X., ZHANG, Y., NASSAR, M., BURNSTOCK, G. & SCHOEPFER, R. (1995). A P2X purinoceptor cDNA conferring a novel pharmacological profile. *FEBS Lett.,* **375,** 129–133.

BRAKE, A.J., WAGENBACH, M.J. & JULIUS, D. (1994). New structural motif for ligand-gated ion channels defined by an ionotropic ATP receptor. *Nature,* **371,** 519–523.

BUELL, G., MICHEL, A.D., LEWIS, C., COLLO, G., HUMPHREY, P.P.A. & SURPRENANT, A. (1996). $P2X_1$ receptor activation in HL60 cells. *Blood,* **87,** 2659–2664.

BURNSTOCK, G. (2001). Purine-mediated signalling in pain and visceral perception. *Trends Pharmacol. Sci.,* **22,** 182–188.

CAVALIERE, F., FLORENZANO, F., AMADIO, S., FUSCO, F.R., VISCOMI, M.T., D'AMBROSI, N., VACCA, F., SANCESARIO, G., BERNARDI, G., MOLINARI, M. & VOLONTÈ, C. (2003). Up-regulation of $P2X_2$, $P2X_4$ receptor and ischemic cell death: prevention by P2 antagonists. *Neuroscience,* **120,** 85–98.

COLLO, G., NORTH, R.A., KAWASHIMA, E., MERLO-PICH, E., NEIDHART, S., SURPRENANT, A. & BUELL, G. (1996). Cloning of $P2X_5$ and $P2X_6$ receptors and the distribution and properties of an extended family of ATP-gated ion channels. *J. Neurosci.,* **16,** 2495–2507.

DEUTSCH, C. (2003). The birth of a channel. *Neuron,* **40,** 265–276.

EDWARDS, F.A., GIBB, A.J. & COLQUHOUN, D. (1992). ATP receptor-mediated synaptic currents in the central nervous system. *Nature,* **359,** 144–147.

FRANKE, H., KITTNER, H., GROSCHE, J. & ILLES, P. (2003). Enhanced $P2Y_1$ receptor expression in the brain after sensitisation with *d*-amphetamine. *Psychopharmacology,* **167,** 187–194.

FREDHOLM, B.B., ABBRACCHIO, M.P., BURNSTOCK, G., DALY, J.W., HARDEN, T.K., JACOBSON, K.A., LEFF, P. & WILLIAMS, M. (1994). Nomenclature and classification of purinoceptors. *Pharmacol. Rev.,* **46,** 143–156.

FUJII, S., KATO, H. & KURODA, Y. (2002). Cooperativity between extracellular adenosine 5′-triphosphate and activation of *N*-methyl-D-aspartate receptors in long-term potentiation induction in hippocampal CA1 neurons. *Neuroscience,* **113,** 617–628.

IKEUCHI, Y. & NISHIZAKI, T. (1995). ATP-evoked potassium currents in rat striatal neurons are mediated by a P_2 purinergic receptor. *Neurosci. Lett.,* **190,** 89–92.

ILLES, P. & RIBEIRO, J.A. (2004). Molecular physiology of P2 receptors in the central nervous system. *Eur. J. Pharmacol.,* **483,** 5–17.

IZANT, J.G. & McINTOSH, J.R. (1980). Microtubule-associated proteins: a monoclonal antibody to MAP2 binds to differentiated neurons. *Proc. Natl. Acad. Sci. U.S.A,* **77,** 4741–4745.

JAMES, S. & RICHARDSON, P.J. (1993). Production of adenosine from extracellular ATP at the striatal cholinergic synapse. *J. Neurochem.,* **60,** 219–227.

JANG, I.S., RHEE, J.S., KUBOTA, H., AKAIKE, N. & AKAIKE, N. (2001). Developmental changes in P2X purinoceptors on glycinergic presynaptic nerve terminals projecting to rat substantia gelatinosa neurones. *J. Physiol.,* **536,** 505–519.

KANJHAN, R., HOUSLEY, G.D., BURTON, L.D., CHRISTIE, D.L., KIPPENBERGER, A., THORNE, P.R., LUO, L. & RYAN, A.F. (1999). Distribution of the $P2X_2$ receptor subunit of the ATP-gated ion channels in the rat central nervous system. *J. Comp. Neurol.,* **407,** 11–32.

KAWAGUCHI, Y. (1992). Large aspiny cells in the matrix of the rat neostriatum *in vitro*: physiological identification, relation to the compartments and excitatory postsynaptic currents. *J. Neurophysiol.,* **67,** 1669–1682.

KAWAGUCHI, Y. (1993). Physiological, morphological, and histochemical characterization of three classes of interneurons in rat neostriatum. *J. Neurosci.,* **13,** 4908–4923.

KAWAGUCHI, Y., WILSON, C.J., AUGOOD, S.J. & EMSON, P.C. (1995). Striatal interneurones: chemical, physiological and morphological characterization. *Trends Neurosci.,* **18,** 527–535.

KHAKH, B.S. (2001). Molecular physiology of P2X receptors and ATP signalling at synapses. *Nat. Rev. Neurosci.,* **2,** 165–174.

KHAKH, B.S., BURNSTOCK, G., KENNEDY, C., KING, B.F., NORTH, R.A., SÉGUÉLA, P., VOIGT, M. & HUMPHREY, P.P.A. (2001). International Union of Pharmacology. XXIV. Current status of the nomenclature and properties of P2X receptors and their subunits. *Pharmacol. Rev.,* **53,** 107–118.

KIDD, E.J., GRAHAMES, C.B.A., SIMON, J., MICHEL, A.D., BARNARD, E.A. & HUMPHREY, P.P.A. (1995). Localization of P_{2X} purinoceptor transcripts in the rat nervous system. *Mol. Pharmacol.,* **48,** 569–573.

LAMBRECHT, G., FRIEBE, T., GRIMM, U., WINDSCHEIF, U., BUNGARDT, E., HILDEBRANDT, C., BÄUMERT, H.G., SPATZ-KÜMBEL, G. & MUTSCHLER, E. (1992). PPADS, a novel functionally selective antagonist of P_2 purinoceptor-mediated responses. *Eur. J. Pharmacol.,* **217,** 217–219.

LÊ, K.T., VILLENEUVE, P., RAMJAUN, A.R., McPHERSON, P.S., BEAUDET, A. & SÉGUÉLA, P. (1998). Sensory presynaptic and widespread somatodendritic immunolocalization of central ionotropic P2X ATP receptors. *Neuroscience,* **83,** 177–190.

LI, C. (2000). Novel mechanism of inhibition by the P2 receptor antagonist PPADS of ATP-activated current in dorsal root ganglion neurons. *J. Neurophysiol.,* **83,** 2533–2541.

MERCIK, K., ZARNOWSKA, E.D., MANDAT, M. & MOZRZYMAS, J.W. (2002). Saturation and self-inhibition of rat hippocampal $GABA_A$ receptors at high GABA concentrations. *Eur. J. Neurosci.,* **16,** 2253–2259.

MOORE, D.J., CHAMBERS, J.K., WAHLIN, J.P., TAN, K.B., MOORE, G.B., JENKINS, O., EMSON, P.C. & MURDOCK, P.R. (2001). Expression pattern of human P2Y receptor subtypes: a quantitative reverse transcription-polymerase chain reaction study. *Biochim. Biophys. Acta,* **1521,** 107–119.

MOORE, D., CHAMBERS, J., WALDVOGEL, H., FAULL, R. & EMSON, P. (2000). Regional and cellular distribution of the $P2Y_1$ purinergic receptor in the human brain: striking neuronal localisation. *J. Comp. Neurol.,* **421,** 374–384.

NICKE, A., RETTINGER, J. & SCHMALZING, G. (2003). Monomeric and dimeric byproducts are the principal functional elements of higher order $P2X_1$ concatamers. *Mol. Pharmacol.,* **63,** 243–252.

NIEBER, K., POELCHEN, W. & ILLES, P. (1997). Role of ATP in fast excitatory synaptic potentials in locus coeruleus neurones of the rat. *Br. J. Pharmacol.,* **122,** 423–430.

NÖRENBERG, W. & ILLES, P. (2000). Neuronal P2X receptors: localisation and functional properties. *Naunyn-Schmiedeberg's Arch. Pharmacol.,* **362,** 324–339.

NÖRENBERG, W., SCHÖFFEL, E., SZABO, B. & STARKE, K. (1997a). Subtype determination of soma-dendritic α_2-autoreceptors in slices of rat locus coeruleus. *Naunyn-Schmiedeberg's Arch. Pharmacol.,* **356,** 159–165.

NÖRENBERG, W., WIRKNER, K. & ILLES, P. (1997b). Effect of adenosine and some of its structural analogues on the conductance of NMDA receptor channels in a subset of rat neostriatal neurones. *Br. J. Pharmacol.,* **122,** 71–80.

NORTH, R.A. (2002). Molecular physiology of P2X receptors. *Physiol. Rev.,* **82,** 1013–1067.

PANKRATOV, Y., CASTRO, E., MIRAS-PORTUGAL, M.T. & KRISHTAL, O. (1998). A purinergic component of the excitatory postsynaptic current mediated by P2X receptors in the CA1 neurons of the rat hippocampus. *Eur. J. Neurosci.,* **10,** 3898–3902.

PANKRATOV, Y., LALO, U., KRISHTAL, O. & VERKHRATSKY, A. (2002). Ionotropic P2X purinoreceptors mediate synaptic transmission in rat pyramidal neurones of layer II/III of somato-sensory cortex. *J. Physiol.,* **542,** 529–536.

PÉREZ-OTAÑO, I., SCHULTEIS, C.T., CONTRACTOR, A., LIPTON, S.A., TRIMMER, J.S., SUCHER, N.J. & HEINEMANN, S.F. (2001). Assembly with the NR1 subunit is required for surface expression of NR3A-containing NMDA receptors. *J. Neurosci.,* **21,** 1228–1237.

PLENZ, D. & KITAI, S.T. (1998). Up and down states in striatal medium spiny neurons simultaneously recorded with spontaneous activity in fast-spiking interneurons studied in cortex-striatum-substantia nigra organotypic cultures. *J. Neurosci.,* **18,** 266–283.

RICHARDSON, P.J. & BROWN, S.J. (1987). ATP release from affinity-purified rat cholinergic nerve terminals. *J. Neurochem.,* **48,** 622–630.

ROYLE, S.J., BOBANOVIC, L.K. & MURRELL-LAGNADO, R.D. (2002). Identification of a non-canonical tyrosine-based endocytic motif in an ionotropic receptor. *J. Biol. Chem.,* **277,** 35378–35385.

RYU, J.K., KIM, J., CHOI, S.H., OH, Y.J., LEE, Y.B., KIM, S.U. & JIN, B.K. (2002). ATP-induced *in vivo* neurotoxicity in the rat striatum *via* P2 receptors. *Neuroreport,* **13,** 1611–1615.

SAK, K. & WEBB, T.E. (2002). A retrospective of recombinant P2Y receptor subtypes and their pharmacology. *Arch. Biochem. Biophys.,* **397,** 131–136.

SATHER, W., DIEUDONNÉ, S., MACDONALD, J.F. & ASCHER, P. (1992). Activation and desensitization of *N*-methyl-D-aspartate receptors in nucleated outside-out patches from mouse neurones. *J. Physiol.,* **450,** 643–672.

SCHEIBLER, P., WIRKNER, K., PESIC, M., ILLES, P. & NÖRENBERG, W. (2002). Effects of extracellular ATP in the rat neostriatum. *Naunyn-Schmiedeberg's Arch. Pharmacol.,* **365,** R32.

SHEN, K.Z. & NORTH, R.A. (1993). Excitation of rat locus coeruleus neurons by adenosine 5′-triphosphate: ionic mechanism and receptor characterization. *J. Neurosci.,* **13,** 894–899.

TEPPER, J.M., SHARPE, N.A., KOÓS, T.Z. & TRENT, F. (1998). Postnatal development of the rat neostriatum: electrophysiological, light- and electron-microscopic studies. *Dev. Neurosci.,* **20,** 125–145.

TORRES, G.E., EGAN, T.M. & VOIGT, M.M. (1999). Hetero-oligomeric assembly of P2X receptor subunits. *J. Biol. Chem.,* **274,** 6653–6659.

TRENDELENBURG, A.U. & BÜLTMANN, R. (2000). P2 receptor-mediated inhibition of dopamine release in rat neostriatum. *Neuroscience,* **96,** 249–252.

TSCHÖPL, M., HARMS, L., NÖRENBERG, W. & ILLES, P. (1992). Excitatory effects of adenosine 5'-triphosphate on rat locus coeruleus neurones. *Eur. J. Pharmacol.,* **213,** 71–77.

VON KÜGELGEN, I. & WETTER, A. (2000). Molecular pharmacology of P2Y-receptors. *Naunyn-Schmiedeberg's Arch. Pharmacol.,* **362,** 310–323.

WAN, X., JURANKA, P. & MORRIS, C.E. (1999). Activation of mechanosensitive currents in traumatized membrane. *Am. J. Physiol.,* **276,** C318–C327.

WELFORD, L.A., CUSACK, N.J. & HOURANI, S.M.O. (1987). The structure–activity relationships of ectonucleotidases and of excitatory P_2-purinoceptors: evidence that dephosphorylation of ATP analogues reduces pharmacological potency. *Eur. J. Pharmacol.,* **141,** 123–130.

WIRKNER, K., FRANKE, H., INOUE, K. & ILLES, P. (1998). Differential age-dependent expression of α_2 adrenoceptor- and P2 purinoceptor-functions in rat locus coeruleus neurons. *Naunyn-Schmiedeberg's Arch. Pharmacol.,* **357,** 186–189.

YAO, S.T., BARDEN, J.A., FINKELSTEIN, D.I., BENNETT, M.R. & LAWRENCE, A.J. (2000). Comparative study on the distribution patterns of $P2X_1$–$P2X_6$ receptor immunoreactivity in the brainstem of the rat and the common marmoset (*Callithrix jacchus*): association with catecholamine cell groups. *J. Comp. Neurol.,* **427,** 485–507.

ZHANG, J., KORNECKI, E., JACKMAN, J. & EHRLICH, Y.H. (1988). ATP secretion and extracellular protein phosphorylation by CNS neurons in primary culture. *Brain Res. Bull.,* **21,** 459–464.

ZIMMERMANN, H. (1999). Two novel families of ectonucleotidases: molecular structures, catalytic properties and a search for function. *Trends Pharmacol. Sci.,* **20,** 231–236.

(Received February 24, 2004
Revised May 28, 2004
Accepted June 10, 2004)